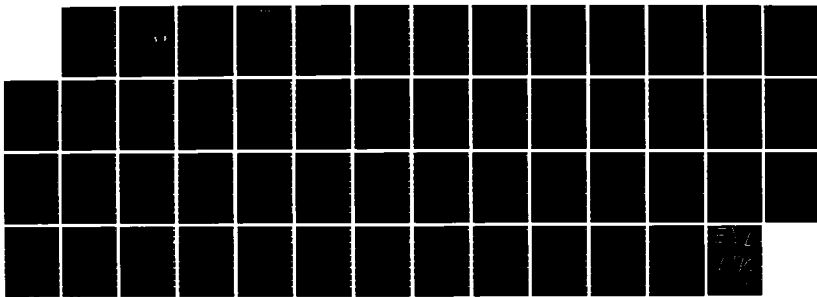
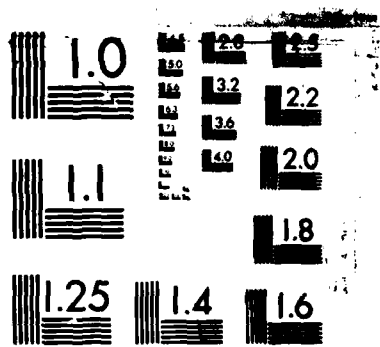


RD-A167 467 ELECTRODYNAMIC SIMILITUDE AND PHYSICAL SCALE MODELING 1/1
PART 1 NONDISPERSIVE TARGETS(U) DAVID W TAYLOR NAVAL
SHIP RESEARCH AND DEVELOPMENT CENTER BET..
UNCLASSIFIED C R SCHUMACHER APR 86 DTNSRDC-86/823 F/G 20/3 NL





MICROCOPY RESOLUTION TEST CHART
NATIONAL BUREAU OF STANDARDS 403 A

DTNSRDC-86/023

12

DAVID W. TAYLOR NAVAL SHIP RESEARCH AND DEVELOPMENT CENTER

Bethesda, Maryland 20084



ELECTRODYNAMIC SIMILITUDE AND PHYSICAL SCALE MODELING

AD-A167 467

PART I: NONDISPERSIVE TARGETS

by

Clifford R. Schumacher

DTIC ELECTED MAY 05 1986
S D
A P

APPROVED FOR PUBLIC RELEASE; DISTRIBUTION UNLIMITED.

DTIC FILE COPY

CENTRAL INSTRUMENTATION DEPARTMENT
RESEARCH AND DEVELOPMENT REPORT

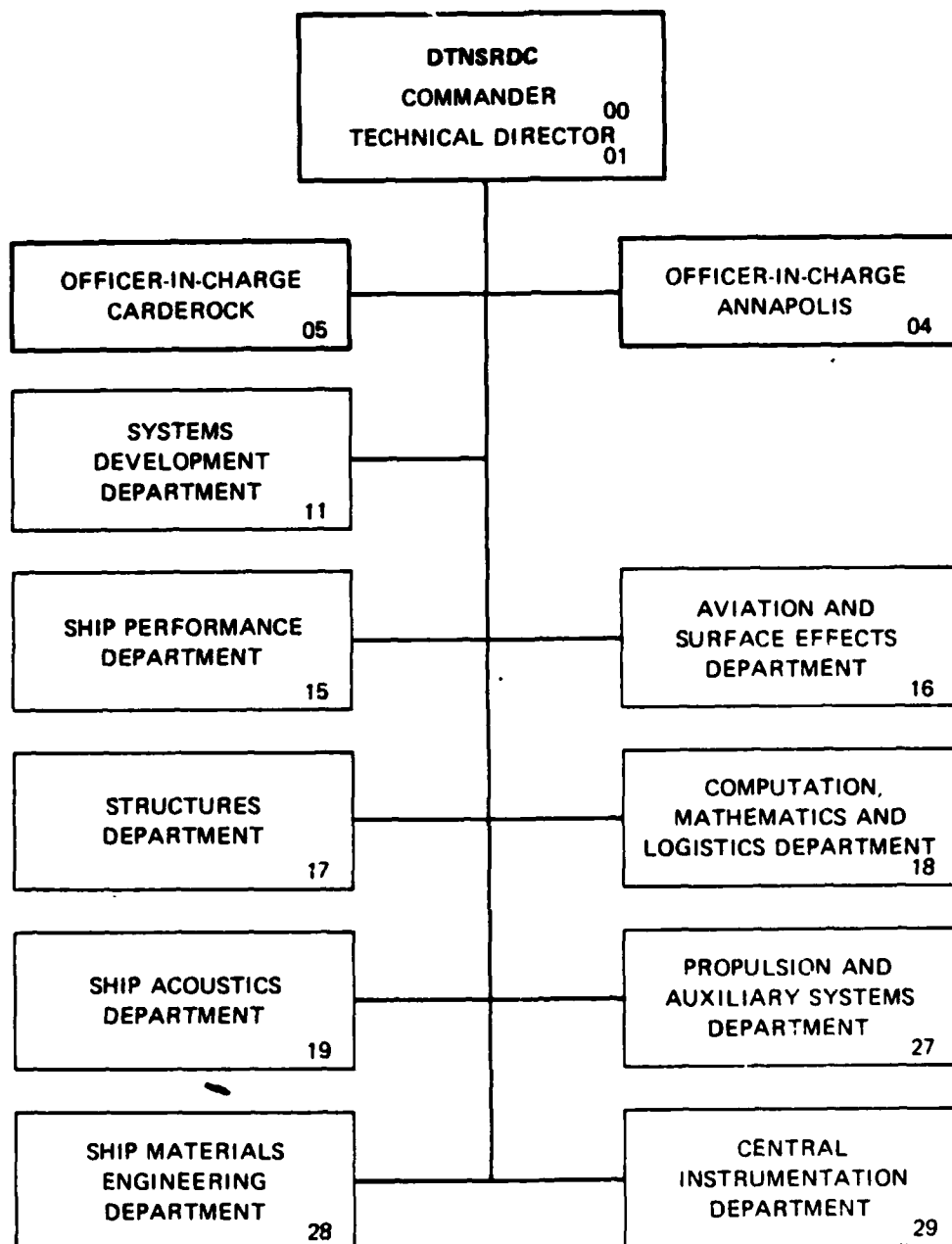
ELECTRODYNAMIC SIMILITUDE AND PHYSICAL SCALE MODELING
PART I: NONDISPERSIVE TARGETS

APRIL 1986

DTNSRDC-86/023

86 5 005

MAJOR DTNSRDC ORGANIZATIONAL COMPONENTS



UNCLASSIFIED

SECURITY CLASSIFICATION OF THIS PAGE

AD-1169469

REPORT DOCUMENTATION PAGE

1a REPORT SECURITY CLASSIFICATION Unclassified		1b RESTRICTIVE MARKINGS	
2a SECURITY CLASSIFICATION AUTHORITY		3 DISTRIBUTION AVAILABILITY OF REPORT APPROVED FOR PUBLIC RELEASE; DISTRIBUTION UNLIMITED.	
2b DECLASSIFICATION/DOWNGRADING SCHEDULE			
4 PERFORMING ORGANIZATION REPORT NUMBER(S) DTNSRDC-86/023		5 MONITORING ORGANIZATION REPORT NUMBER(S)	
6a NAME OF PERFORMING ORGANIZATION David Taylor Naval Ship R&D Center	6b OFFICE SYMBOL (If applicable) Code 2930	7a NAME OF MONITORING ORGANIZATION DTNSRDC Research Coordinator Code 012.3	
6c ADDRESS (City, State, and ZIP Code) Bethesda, Md. 20084-5000		7b ADDRESS (City, State, and ZIP Code) Bethesda, Md. 20084-5000	
8a NAME OF FUNDING SPONSORING ORGANIZATION Chief of Naval Research	8b OFFICE SYMBOL (If applicable) OCNR 300	9 PROCUREMENT INSTRUMENT IDENTIFICATION NUMBER	
10 SOURCE OF FUNDING NUMBERS PROGRAM ELEMENT NO 62766N		PROJECT NO F66412	TASK NO NOZF-66-412-001
11 SOURCE OF FUNDING NUMBERS WORK UNIT ACCESSION NO DN479603			
12 PERSONAL AUTHOR(S) Clifford R. Schumacher			
13 DATE OF REPORT Research & Development	13b TIME COVERED FROM 831001 to 851001	14 DATE OF REPORT (Year, Month, Day) April 1986	15 PAGE COUNT 51
16 SUPPLEMENTARY NOTATION			
17a	17b USAGF CODES GROUP	18 SUBJECT TERMS (Continue on reverse if necessary and identify by block number) Silencing (Non Acoustic), Electromagnetic, Radar, Physical Scale Modeling, Maxwell's Equations	
19a ABSTRACT (Continue on reverse if necessary and identify by block number) This report presents a complete and rigorous treatment of the predictions of electrodynamic similitude relating scattering from scaled targets to scattering from full-size targets. The usual assumption is made that the targets' treated are those whose conductivity, permittivity, and permeability do not change with frequency. Three general nonlinear modeling equations in six variables are derived, and a complete set of solutions is presented. For the first time, particular emphasis is given to the effects of differences between geometric and complete scaling on the electromagnetic fields and on the radar cross section, and effects of approximations to complete scaling are evaluated. Conditions are obtained on properties of materials required for models made from these materials to accurately simulate systems. Absorption and energy balance are also treated, and the influence of finite conductivity on surface currents is shown.			
19b		(Continued)	
20 DISTRIBUTION AVAILABILITY OF ABSTRACT <input checked="" type="checkbox"/> UNCLASSIFIED / UNLIMITED <input type="checkbox"/> SAME AS PDT <input type="checkbox"/> DTC USERS		21 ABSTRACT SECURITY CLASSIFICATION Unclassified	
22a NAME OF RESPONSIBLE INDIVIDUAL Clifford R. Schumacher		22b TELEPHONE (Include Area Code) (301) 267-2352	22c OFFICE SYMBOL Code 2930

UNCLASSIFIED

SECURITY CLASSIFICATION OF THIS PAGE

(Block 19 Continued)

The possibility of using scaled down models of real targets is usually claimed to be based on the linearity of Maxwell's equations. Therefore, we first examined the physics involved in linearity, its relation to the Maxwell equations in macroscopic media, and its impact on physical scale modeling. The behavior of electromagnetic fields was also examined as a function of frequency. Upper bounds on the electric conductivity and limitations on the electric and magnetic polarizability of realistic materials may have profound implications for model measurements. All the energy density in the reflected wave may be lost at higher frequencies by incomplete scaling of even apparently nonabsorptive targets. Thus, the ratio of measured radar cross sections of geometrically scaled targets to those predicted for a completely scaled model will eventually approach zero.

11
UNCLASSIFIED

SECURITY CLASSIFICATION OF THIS PAGE

TABLE OF CONTENTS

	Page
NOTATION	iv
ABSTRACT	1
ADMINISTRATIVE INFORMATION	1
INTRODUCTION	1
THE MAXWELL EQUATIONS IN MACROSCOPIC MATERIALS	4
IMPACT OF LINEARITY ON PHYSICAL SCALE MODELING	6
NONLOCALITY IN SPACE AND TIME	8
ENTRANCE OF THE SKIN DEPTH.	9
NONLINEAR OPTICS.	14
MODELING OF ELECTROMAGNETIC SYSTEMS.	14
SOLUTIONS OF THE MODELING EQUATIONS.	18
GENERAL SOLUTION.	18
FINITE CONDUCTIVITY AND SURFACE CURRENTS.	20
DIFFERENCES BETWEEN GEOMETRIC AND COMPLETE SCALING.	22
CONDITIONS FOR AN ABSOLUTE MODEL.	24
ABSORPTION IN NONDISPERSIVE TARGETS.	25
ELECTRIC AND MAGNETIC SCATTERING.	27
PLANE WAVES IN DISSIPATIVE MATERIALS.	29
SCALING OF THE SCATTERING CROSS SECTION	31
ENERGY BALANCE AND DEPENDENCE ON FREQUENCY	33
SUMMARY AND CONCLUSIONS.	35
RECOMMENDATIONS.	36
ACKNOWLEDGMENTS.	37
REFERENCES	39

NOTATION

a	Area
\bar{B}	Magnetic flux density (or magnetic induction) vector
c	Velocity of light in free space
\bar{D}	Electric displacement vector
\bar{E}	Electric field intensity vector (in original medium)
\bar{E}'	Electric field intensity vector in model
e	Ratio of model characteristic electric field intensities to those in original medium
f	Frequency (and, including and following Equation (10c), ratio of model to original frequencies)
\bar{H}	Magnetic field intensity vector (in original medium)
\bar{H}'	Magnetic field intensity vector in model
\bar{H}_t	Tangential component of magnetic field intensity vector
h	Ratio of model characteristic magnetic field intensities to those in original medium
i	$\sqrt{-1}$
\bar{J}	Free electric current density vector
k	Propagation constant of light when $\sigma = 0$
L	Characteristic length (in original system)
L'	Characteristic length in model
λ	Ratio of model characteristic lengths to those in original system
\bar{M}	Induced magnetization vector
\bar{P}	Induced electric polarization vector
P	Time-average electromagnetic power absorbed
p	Mechanical scale factor (reciprocal of λ)
\bar{S}	Poynting Vector ($\bar{S} = \bar{E} \times \bar{H}$)
T	Ratio of model characteristic times to those in original system

t Characteristic time (in original system)
 t' Characteristic time in model
 v Velocity of light in a material medium ($v = 1/\sqrt{\epsilon\mu}$)
 x,y,z Rectangular Cartesian coordinates of a point in space
 Z Complex characteristic (or wave) impedance of a medium
 Z' Real part of the characteristic impedance (resistance)
 Z" Imaginary part of the characteristic impedance (reactance)
 Z₀ Characteristic impedance of a medium when $\sigma = 0$
 α Real part of the complex propagation constant or attenuation constant
 β Imaginary part of the complex propagation constant (= k when $\sigma = 0$)
 γ Complex propagation constant
 δ Skin depth
 ∂ Partial derivative operator
 ϵ Electric permittivity (dielectric constant) in original medium (and, following Equations (13a), ratio of model to original permittivity)
 ϵ' Electric permittivity in model
 ϵ_0 Electric permittivity of free space
 ζ Ratio of model characteristic impedances to those in original medium
 n Electric loss tangent
 κ_e Electric permittivity relative to free space
 κ_m Magnetic permeability relative to free space
 λ Wavelength
 μ Magnetic permeability in original medium (and, following Equations (13a), ratio of model to original permeability)
 μ' Magnetic permeability in model
 μ_0 Magnetic permeability of free space
 π Pi (3.141592654)
 ρ Free charge density

Accession For	
NTIS	CRA&I
DTIC	TAB
Unannounced	
Justification	
By _____	
Distribution /	
Availability Codes	
Dist	Avail and/or Special
1-1	24



σ	Electric conductivity in original medium (and, following Equations (13a), ratio of model to original conductivity)
σ'	Electric conductivity in model
χ_e	Electric susceptibility
χ_m	Magnetic susceptibility
ω	Angular frequency ($= 2\pi f$)
$\bar{\nabla} \cdot$	Divergence operator (div)
$\bar{\nabla} \times$	Curl operator
∇^2	Laplacian operator (div(grad))

ABSTRACT

This report presents a complete and rigorous treatment of the predictions of electrodynamic similitude relating scattering from scaled targets to scattering from full-size targets. The usual assumption is made that the targets treated are those whose conductivity, permittivity, and permeability do not change with frequency. Three general nonlinear modeling equations in six variables are derived, and a complete set of solutions is presented. For the first time, particular emphasis is given to the effects of differences between geometric and complete scaling on the electromagnetic fields and on the radar cross section, and effects of approximations to complete scaling are evaluated. Conditions are obtained on properties of materials required for models made from these materials to accurately simulate systems. Absorption and energy balance are also treated, and the influence of finite conductivity on surface currents is shown.

The possibility of using scaled-down models of real targets is usually claimed to be based on the linearity of Maxwell's equations. Therefore, we first examined the physics involved in linearity, its relation to the Maxwell equations in macroscopic media, and its impact on physical scale modeling. The behavior of electromagnetic fields was also examined as a function of frequency. Upper bounds on the electric conductivity and limitations on the electric and magnetic polarizability of realistic materials may have profound implications for model measurements. All the energy density in the reflected wave may be lost at higher frequencies by incomplete scaling of even apparently nonabsorptive targets. Thus, the ratio of measured radar cross sections of geometrically scaled targets to those predicted for a completely scaled model will eventually approach zero.

ADMINISTRATIVE INFORMATION

This project was supported by the DTNSRDC Independent Exploratory Development Program, sponsored by the Office of Chief of Naval Research, Director of Navy Laboratories, OCNR 300 and administered by the Research Coordinator, DTNSRDC 012.3 under Program Element 62766N, Task Area ZF-66-412-001 under DTNSRDC Work Unit 1-2930-001.

INTRODUCTION

The recent development of millimeter and submillimeter and of infrared and

visible laser (lidar) radar systems for detection of military vehicles [1]* has stimulated considerable interest in scaled-down models of radar targets. The distribution of radiation scattered from a full-size target is expected to be predictable from measurements on a faithful scale model.

Models of electromagnetic systems have been used for antenna studies [2] since the early 1900's. However, the earliest known work on model measurements of radar cross sections (RCS) was at Massachusetts Institute of Technology Radiation Laboratory in 1942 [3]. This application received considerable impetus from the suggestions and work of Sinclair and his colleagues during World War II [4, 5], and has been extensively pursued since then [6-12]. Despite some problems in preparing the models themselves and in making measurements, scale models provide an important means both of determining the RCS of targets for which no other method is practical and of providing independent verification of values found in other ways.

Scale models of physical systems all depend on principles of similitude which allow relationships to be established between model and full-scale behavior. Equations for scaling electromagnetic models have previously been written by Stratton [13], Brown and King [14, 15], and Sinclair [5]. However, practical difficulties with scaling properties of realistic materials now exist which, for most scattering measurements, discourage all but simple geometric scaling [1, 9-12, 16-18]. Geometric scaling is a partial form of scaling, where the scaled target has the same dimensions in scaled wavelengths as the actual target has in actual wavelengths, but material properties are ignored.

Since a complete set of solutions to the general scaling equations has never previously been published, little concern was shown about differences between geometric and complete scaling in radar applications [1]. Although it has been known that scaled electric conductivity (σ) should increase with frequency (f),

* References are listed on page 39.

differences between surface current distributions on poor conductors and on perfectly conducting targets were believed to be unimportant. Thus, infinite σ is usually assumed, the f -dependence of material properties is usually ignored, and little attention has been given to resulting differences in the electromagnetic fields involved.

However, this report will show this lack of concern is not justified. Here, we develop a complete and rigorous treatment of the relations between scattering from scaled and full-size targets on the basis of electrodynamic similitude, starting with the usual assumption that not only σ but also electric permittivity (dielectric constant) (ϵ) and magnetic permeability (μ) do not change with f . Three general nonlinear modeling equations in six variables are derived, and a complete set of solutions is presented. For the first time, particular emphasis is given to effects of differences between geometric and complete scaling on the electromagnetic fields involved and on the RCS, and effects of approximations to complete scaling are evaluated. Conditions are obtained on properties of materials required for models made from these materials to accurately simulate systems. Absorption and energy balance are also treated, and the influence of finite σ on surface currents is shown.

The possibility of using scaled-down models of real targets is usually claimed to be based on linearity of Maxwell's equations [6, 10-12]. Thus, we first examine the physics involved in linearity, its relation to the Maxwell equations in macroscopic media, and its impact on physical scale modeling.

The behavior of electromagnetic fields is also examined as a function of frequency. Unfortunately, it is physically impossible to satisfy scaling conditions exactly when realistic materials are used and the change in f is appreciable, because this would require that upper bounds on physical σ be exceeded at higher f , and definite limitations also exist on physical ϵ and μ .

This report will show that incomplete scaling of apparently nonabsorptive targets may have profound implications for model measurements. Both electric and magnetic scattering are considered. The energy density in the reflected wave will be examined at higher frequencies for both geometrically and completely scaled targets, and the frequency dependence of the RCS measured for geometrically scaled targets will be compared to that predicted for a completely scaled model.

THE MAXWELL EQUATIONS IN MACROSCOPIC MATERIALS

All scattering characteristics, including interference and diffraction, polarization, and creeping and traveling (surface) wave phenomena, should be correctly represented by rigorous scale modeling.

If the model is to be an accurate simulation of a full-scale system, transformations relating model to full-scale quantities will transform Maxwell's equations from model to full-scale systems. Since electromagnetic fields in both systems must satisfy Maxwell's equations, we can thereby determine how ϵ , μ , and σ must transform for simulation to be accurate. However, because upper bounds on electric conductivity and limitations on electric and magnetic polarizability sometimes render complete scaling impossible, approximations to complete scaling should be investigated.

To examine the origin and impact of these approximations, we must start from the Maxwell equations in macroscopic materials. Following the rationalized Meter-Kilogram-Second-Ampere (MKSA) system of units used by Stratton [13], these relations can be written

$$\bar{\nabla} \times \bar{E} = - \frac{\partial \bar{B}}{\partial t} \quad (1a)$$

$$\bar{\nabla} \cdot \bar{B} = 0 \quad (1b)$$

and

$$\bar{\nabla} \times \bar{H} = \bar{J} + \frac{\partial \bar{D}}{\partial t} \quad (2a)$$

$$\bar{\nabla} \cdot \bar{D} = \rho \quad (2b)$$

where

\bar{E} = electric field intensity (V/m)

\bar{B} = magnetic induction (T or Wb/m²)

\bar{H} = magnetic field intensity (A/m)

\bar{D} = electric displacement (C/m²)

\bar{J} = free electric current density (A/m²)

ρ = free charge density (C/m³)

and the vector operators ($\bar{\nabla} \times$ and $\bar{\nabla} \cdot$) are used to indicate how changes in space of the above quantities are coupled to their changes in time (t).

\bar{E} and \bar{B} are macroscopic electric and magnetic field quantities, averaged over volumes which are large compared to the volume occupied by a single atom or molecule. \bar{D} and \bar{H} are corresponding derived electric and magnetic fields, related to \bar{E} and \bar{B} through constitutive relations

$$\begin{aligned} \bar{D} &= \bar{D}[\bar{E}, \bar{B}] \\ \bar{H} &= \bar{H}[\bar{E}, \bar{B}] \end{aligned} \quad (3)$$

Square brackets are used to signify functional relations that are not necessarily simple, because they may depend on past history (hysteresis), may reflect the derived polarization fields' lagging behind the changes in source fields causing these effects, may be nonlinear, or some other factor.

The two homogeneous equations, Equations (1a) and (1b), can be solved formally by expressing \bar{E} and \bar{B} in terms of scalar and vector potentials, but the two inhomogeneous equations, Equations (2a) and (2b), cannot be solved until the derived fields \bar{D} and \bar{H} are known in terms of \bar{E} and \bar{B} . Bound charges and currents enter Equations (3) through these derived fields, which represent macroscopically

averaged electric and magnetic dipole, electric and magnetic quadrupole, and higher moment densities of material media induced by applied fields.

In addition, forces on electrons depend on both magnetic and electric fields, so for currents in conducting materials there is a generalized Ohm's law,

$$\bar{J} = \bar{J}[\bar{E}, \bar{B}] \quad (4)$$

In most materials, only electric and magnetic polarizations \bar{P} and \bar{M} are significant. Then, electric quadrupole and higher terms in Equations (3) are completely negligible, and we may define

$$\begin{aligned}\bar{D} &= \epsilon_0 \bar{E} + \bar{P} \\ \bar{B} &= \mu_0 (\bar{H} + \bar{M})\end{aligned} \quad (5)$$

where

\bar{P} = induced electric polarization (C/m^2)

\bar{M} = induced magnetization (A/m)

ϵ_0 = permittivity of vacuum = 8.854 pF/m

μ_0 = permeability of vacuum = $400\pi \text{ nH/m}$

These equations form the basis of all classical electromagnetic phenomena. When they are combined with the Lorentz force equation and Newton's laws of classical mechanics to describe coupling between the fields and their moving sources, they provide a complete description of the classical dynamics of interacting charged particles and electromagnetic fields [19].

IMPACT OF LINEARITY ON PHYSICAL SCALE MODELING

The claim that scaled-down models can be used to simulate real targets is based on linearity of Maxwell's equations [6, 10-12]. Hence, our treatment does not apply to obviously nonlinear materials, such as ferromagnetic materials and ionized regions with magnetic fields. However, the impact of linearity on other types of physical scale models deserves some clarification.

The Maxwell equations are linear partial differential equations. Since they are linear in the fields, these only appear to the first power, and linear superposition holds. Therefore, any sum of solutions of Maxwell's equations is also a solution.

However, nonlinear effects may intrude in physical scale modeling, and it is helpful to distinguish between the trivial linearity of equations, the more complicated linear response of electrical devices, and the still subtler linearity of materials. Common examples of transitions from the linear to the nonlinear regime occur in transducers used to couple telephone conversations with a microwave beam, in crystals responding to intense laser beams, and in magnetic materials.

The constitutive relations, Equations (5), permit a simple definition of the linear response of a medium. Accordingly, materials are termed linear when an applied \bar{E} or \bar{H} field induces a \bar{P} or \bar{M} polarization, respectively, that is proportional to the magnitude of the applied field. Thus, our treatment also does not apply to substances where \bar{P} or \bar{M} is not proportional to the magnitude of the applied field, such as ferroelectrics or ferromagnets, which have nonzero \bar{P} or \bar{M} in the absence of any applied fields.

The Maxwell equations are valid for nonhomogeneous as well as for homogeneous materials. For weak enough fields, however, different Cartesian components of \bar{E} and \bar{D} and of \bar{B} and \bar{H} are coupled through the electric permittivity or dielectric tensor, and through the magnetic permeability tensor, respectively. These tensors summarize the linear response of the medium and are dependent on molecular and, perhaps, crystalline structure of the material, as well as on such bulk properties as density and temperature.

For simple materials, this linear response may be isotropic in space, whereupon the tensors become diagonal with all three elements equal. Equations (5) then become

$$\begin{aligned}\bar{D} &= \epsilon_0 \bar{E} + \chi_e \epsilon_0 \bar{E} = \epsilon_0 (1 + \chi_e) \bar{E} = \kappa_e \epsilon_0 \bar{E} = \epsilon \bar{E} \\ \bar{B} &= \mu_0 (\bar{H} + \chi_m \bar{H}) = \mu_0 (1 + \chi_m) \bar{H} = \kappa_m \mu_0 \bar{H} = \mu \bar{H}\end{aligned}\quad (6)$$

In addition, assuming no Hall or low temperature effects, Equation (4) becomes Ohm's law

$$\bar{J} = \sigma \bar{E} \quad (7)$$

where

χ_e = electric susceptibility (dimensionless)

κ_e = electric permittivity relative to free space (dimensionless)

ϵ = permittivity of medium (F/m)

χ_m = magnetic susceptibility (dimensionless)

κ_m = magnetic permeability relative to free space (dimensionless)

μ = permeability of medium (H/m)

σ = electric conductivity of medium (mho/m)

NONLOCALITY IN SPACE AND TIME

In general, the basic linear connection between \bar{D} and \bar{E} , as well as between \bar{H} and \bar{B} and between \bar{J} and \bar{E} , may be nonlocal. Nonlocality in time and space implies that a principal property of the relations (6) and (7), namely the dependence of \bar{J} , \bar{D} , and \bar{B} only on values of \bar{E} and \bar{H} at the instant or place considered, is no longer true.

In general, the values of \bar{J} , \bar{D} , and \bar{B} at a given instant are determined not only by the values of \bar{E} and \bar{H} at that instant, but also by values of \bar{E} and \bar{H} at every previous instant. Furthermore, with sufficiently rapidly varying applied fields, because of the inertia of electrons and other more massive atomic and molecular solid state constituents, establishment of \bar{P} or \bar{M} polarization in materials and the flow of currents through them will eventually not be able to keep up with the changes in \bar{E} and \bar{H} causing these effects [19-21].

Also, long-range effects may become important, so a spatially local form of

Ohm's law is no longer adequate. Thus, Equations (6) and (7) should be understood as holding for Fourier transforms of the field components in space and time. The permittivity, permeability, and conductivity tensors are then functions of frequency f and wavelength λ [19,20]. Nonlocality in space may often be neglected in conductors up through optical frequencies, as long as the mean free path for conduction electrons colliding with the lattice structure is small compared to the skin depth, whereupon ϵ , μ , and σ become functions only of f in dispersive targets. However, this f dependence can be present down through radar frequencies and it complicates scaling, since ϵ , μ , and σ are complex variables having both real and imaginary (i.e., reflective and absorptive) parts.

ENTRANCE OF THE SKIN DEPTH

When an electromagnetic wave enters a good conductor, its amplitude is a rapidly decreasing function of distance. It is damped to 0.36788 (the reciprocal of the 2.71828 base for natural logarithms) of its initial amplitude in the skin depth δ , where: [13, 19]

$$\delta = \frac{1}{\sqrt{\pi f \sigma \mu}} \quad (8a)$$

σ is also a function of f , so δ decreases as either f or σ increases, approaching zero either when σ becomes very large (perfect conductor) or when f becomes very large. A conductor with vanishing δ would reflect all incident light and would not permit penetration of an electromagnetic wave to any depth at all.

We can understand the electromagnetic fields in the neighborhood of this thin surface layer, as well as the power absorbed in and scattered from it, by considering waves incident on both perfect and good, but not perfect, conductors.

With waves incident on a perfect conductor, the boundary condition associated with Equation (2b) requires that surface charges move instantly in response to

normal \bar{D} outside to produce the correct surface-charge density which gives zero \bar{E} inside. Similarly, in response to tangential \bar{H} outside, the second boundary condition associated with Equation (2a) requires that surface charges move fast enough to produce the correct surface current to give zero \bar{H} inside.

The boundary condition on normal \bar{B} associated with Equation (1b), as well as the other boundary condition on tangential \bar{E} associated with Equation (1a), imply continuity of these two across the surface. Thus, their vanishing values inside require that these two both vanish outside the surface. Therefore, only normal \bar{E} and tangential \bar{H} can exist just outside a perfect conductor, and all fields drop abruptly to zero inside.

For a good, but not perfect, conductor the surface fields and charges behave approximately the same as for a perfect conductor [19, 21]. However, with finite σ , charges and currents do not respond to fields instantaneously, so there is a thin transitional surface layer in which tangential \bar{H} outside undergoes the rapid exponential decay inside that is measured by δ . There is also a normal \bar{E} outside, which undergoes an exponential decay inside similar to tangential \bar{H} , but whose energy density inside is much smaller than the magnetic energy density.

In addition, there are small components of \bar{E} and \bar{H} , tangential and normal to the surface, respectively, outside the conductor. These also decrease exponentially inside, and result in a power flow into the conductor, which can be calculated from Poynting's vector, \bar{S} :

$$\bar{S} = \bar{E} \times \bar{H} \quad (8b)$$

which is the power flow across a unit area normal to \bar{S} , or the energy flux density.

Many such quantities can be shown to be proportional to δ . For example, Panofsky and Phillips have shown [22] that the ratios: (a) of tangential \bar{E} at the metal's surface to its normal component there, as well as (b) of normal \bar{H} to its tangential component there, are both approximately δ/λ .

In addition, the time-average power absorbed (P) per unit area (a) equals the time-average normal component of Poynting's vector [19], which can be written

$$\frac{dP}{da} = \frac{\mu\pi f\delta}{2} |\bar{H}_t|^2 \quad (8c)$$

and thus is proportional to δ . This can also be calculated from ohmic losses due to energy dissipation by the surface currents in the conductor's transition layer. The power absorbed in the conductor leads to a loss of energy in the reflected wave and a decreased scattering cross section.

Therefore, very little power flows into the conductor, to be dissipated there because of wave damping due to development of heat in the surface resistance. Poynting's vector at the surface is very small, since the ratio of \bar{E} to \bar{H} within the metal is much smaller than its value in free space, representing a small energy flow into the metal. The situation is almost like that with a perfect conductor, for which the \bar{E} vectors of the incident and reflected waves are equal in magnitude, but exactly cancel at the metal's surface, whereas the \bar{H} vectors are equal in magnitude, because of the perfect reflection, but add.

For a realistic material such as copper, the above formula for δ becomes

$$\delta = \frac{6.6}{\sqrt{f}} \text{ cm} = \frac{66,000}{\sqrt{f}} \mu\text{m} \quad (8d)$$

yielding $\delta = 0.66 \mu\text{m}$ at $f = 10 \text{ GHz}$, where the $\lambda = 3 \text{ cm}$, and $\delta = 0.047 \mu\text{m}$ at $f = 2000 \text{ GHz}$, where $\lambda = 150 \mu\text{m}$. This rapid attenuation implies that current flows in a rather thin surface layer at high frequencies, and that δ is a very small fraction of λ . Thus, no complicated constructive or destructive interference occurs in this surface layer, and at the metal's surface both tangential \bar{E} and normal \bar{H} are small compared to normal \bar{E} and tangential \bar{H} , respectively, according to the paragraph above Equation (8c).

The above equation will also yield the frequency at which δ and λ eventually become equal:

$$f = \frac{c}{\lambda} = \frac{10^{11}}{4.84} \text{ GHz} = 20.66 \text{ GHz} \quad (8e)$$

where c is the velocity of light (3×10^8 m/sec), and $1 \text{ GHz} = 10^9 \text{ Hz}$. This frequency corresponds to

$$\delta = \lambda = 0.00001452 \mu\text{m} = 0.1452 \text{ \AA} \quad (8f)$$

or about one-quarter the Bohr radius of the hydrogen atom. Both δ and λ appear to be in the quantum mechanical regime, outside the range of classical electromagnetic phenomena.

Although the above conclusions are based on Equation (8a), derived under the assumption $\epsilon\omega \ll \sigma$, where ω is the angular frequency ($= 2\pi f$), dependence on λ becomes important in physical scale models when the mean free path of electrons colliding with the conductor's solid structure becomes comparable to δ , which usually does not occur until one reaches optical frequencies. Then, a spatially local form of Ohm's law is no longer adequate, and long-range effects occur which become important in understanding the surface impedance of metals.

A metal's surface impedance is the ratio of tangential \bar{E} to tangential \bar{H} at its surface. Although its value can be calculated from classical electromagnetic theory, at sufficiently low temperatures the spatial nonuniformity of the electromagnetic fields becomes important. Consequently, a macroscopic description of a metal in terms of ϵ , μ , and σ is no longer possible.

More precisely, as a metal's temperature falls, its σ increases, and an electromagnetic field's depth of penetration into a metal decreases in accordance with the above expressions for δ . At the same time, the amplitude of lattice vibrations decreases with a decrease in temperature, so the electronic collisional mean free path increases and may exceed δ by a large factor. When the mean free

path is comparable with or much greater than δ , electrons will traverse regions with different values of \bar{E} between collisions, and their resultant velocity will depend on the changing values of \bar{E} along the entire path. Since \bar{E} varies over the electron's path, σ is not constant over all parts of the metal, so Ohm's law must be replaced by a more detailed expression where the spatial variation of \bar{E} is taken into account.

The above behavior implies not only that the current at a point depends on the \bar{E} field at other points, but also that the effects of a boundary can be felt at substantial depths. This leads to a nonexponential decay of the field as it penetrates into the medium. These and other departures from the behavior described by the formulas given above for δ are known collectively as the anomalous skin effect [19-21], and can be utilized to map out the energy levels allowed to electrons in metals.

In metals, electrons that have the most available energy, lie on what are called Fermi surfaces. For most electronic properties of metals, the behavior is determined by electron states very near the Fermi surface. This is particularly true with transport properties, for only electrons near the Fermi energy can find an unoccupied state at a nearby energy. Correspondingly, with small applied fields it is only states near this surface for which the occupation number changes. Thus, energy bands in the neighborhood of the Fermi surface are the ones of primary importance.

To summarize, as f increases the classical skin depth decreases. When δ becomes comparable to the mean free path of carriers, we reach the nonlocal regime described above, which usually can be ignored in conductors up through optical frequencies. When δ is much smaller than the carrier mean free path, we encounter what is called the extreme anomalous skin effect. More detailed study of the anomalous skin effect leads to information about the transition between the

classical skin effect and the extreme anomalous region, and to information about details of the shape of the Fermi surface [20].

NONLINEAR OPTICS

Conductors are composed of atoms and molecules bound together in a regular arrangement to form a solid. The electrons in the outer shells of these atoms and molecules can be regarded as being in a potential in which both the electrons and the resulting ions will oscillate linearly at small amplitudes.

Materials showing a linear response to weak electromagnetic fields will eventually show nonlinear behavior at higher field strengths when electronic or ionic oscillators are driven to large amplitudes. A monochromatic wave, when pulsed, develops a spectrum of frequencies which, for large amplitude, may then generate waves in the medium with harmonic, sum and difference, cubic, and higher nonlinear terms, giving rise to a broader spectrum of frequencies. With the development of lasers, such nonlinear behavior has become an active research area, called nonlinear optics [19, 23].

Lasers are capable of generating pulses with peak \bar{E} fields of 10 or even 100 Gigavolts/cm. On the other hand, the static \bar{E} field felt by an electron in the hydrogen atom's ground state is only 5.14 GV/cm, and fields of 100 kV/cm are equal to the average internal fields seen inside a dielectric lattice. Since fields of 100 kV/cm can thus cause electrical breakdown in a solid and destroy it, the laser fields often used with physical scale models may well be capable of driving atomic oscillators into their nonlinear range.

MODELING OF ELECTROMAGNETIC SYSTEMS

Scaling laws result from imposing exact conditions on the Maxwell equations. If a model is to be an accurate simulation of a full-scale system, transformations relating model to full-scale quantities will transform Maxwell's equations from one

system to another. Since electromagnetic fields in both systems must satisfy Maxwell's equations, such a transformation will determine how ϵ , μ , and σ must transform for simulation to be accurate. Replication of each coefficient of the Maxwell equations, considered separately, will then give three general nonlinear modeling equations in six variables.

To obtain these equations, consider a linear, homogeneous, isotropic system with no free charge, where Equations (6) and (7) are valid, and Maxwell's two curl equations, given in Equations (1a) and (2a), take the form

$$\bar{\nabla} \times \bar{E} = -\mu \frac{\partial \bar{H}}{\partial t} \quad (9a)$$

$$\bar{\nabla} \times \bar{H} = \sigma \bar{E} + \epsilon \frac{\partial \bar{E}}{\partial t} \quad (9b)$$

The electromagnetic properties of a configuration of imperfect conductors, dielectrics, and magnetic materials in unbounded space can be compared with the properties of a scale model, which differs geometrically from the original only in having its dimensions changed by a factor λ , which may be larger or smaller than one. If model characteristics are denoted by primes, each model length L' is related to a corresponding length L in the original system according to

$$L' = \lambda L \quad (10a)$$

The conditions imposed by Equation (10a) represent the requirements for a mechanical model of the material portions of a full-scale system, in which there is geometrical similarity in shapes of corresponding material parts. Frequently, a quantity p is defined, the ratio of any full-scale to corresponding model length, called the mechanical scale factor. The parameter p is normally chosen to yield a model of convenient size, would usually be greater than one for smaller models used at higher f , and satisfies

$$p = 1/\lambda \quad (10b)$$

Time is likewise scaled

$$t' = T t = \frac{1}{f} t \quad (10c)$$

where T is the ratio of model characteristic times to those in original system and, since the field's period is inversely proportional to frequency, we redefine f to be the ratio of model to original frequencies.

The requirement that a model's electromagnetic properties shall be the same as those of the original, except for a change of scale, means that the \bar{E} and \bar{H} fields in the space about a model will pick up multiplicative factors

$$\bar{E}' = e \bar{E} \quad \text{and} \quad \bar{H}' = h \bar{H} \quad (11a)$$

where e and h are the ratio of model characteristic electric and magnetic field intensities to those in original medium, respectively. Likewise, ϵ , μ , and σ have new values in the model denoted by primes.

Since Equation (10c) states that all times are to be multiplied by a factor T in a model, first time derivatives may be replaced by

$$\frac{\partial}{\partial t'} = \frac{1}{T} \frac{\partial}{\partial t} = f \frac{\partial}{\partial t} \quad (11b)$$

The curl operator, which involves first derivatives with respect to space coordinates, may similarly be replaced according to Equation (10a). Then, starting with model variables, the Maxwell Equations (9) take the form

$$\begin{aligned} \bar{\nabla}' \times \bar{E}' &= \frac{1}{\epsilon} \bar{\nabla} \times \bar{E}' = - \frac{e}{\epsilon} \bar{\nabla} \times \bar{E} = - \mu' \frac{\partial \bar{H}'}{\partial t'} \\ \bar{\nabla}' \times \bar{H}' &= - \frac{1}{\mu} \bar{\nabla} \times \bar{H}' = - \frac{n}{\mu} \bar{\nabla} \times \bar{H} = \sigma' \bar{E}' + \epsilon' \frac{\partial \bar{E}'}{\partial t'} \end{aligned} \quad (12a)$$

Multiplying the first equation by (ϵ/e) , the second by (μ/h) , and continuing the transformation from primed to unprimed variables

$$\bar{\nabla} \times \bar{E} = -\mu' \frac{\ell}{e} \frac{\partial \bar{H}'}{\partial t} = -\mu' \ell f - \frac{h \frac{\partial \bar{H}}{\partial t}}{e}$$
(12b)

$$\bar{\nabla} \times \bar{H} = \frac{\ell}{h} \left\{ \sigma' \bar{E}' + \epsilon' \frac{\partial \bar{E}'}{\partial t} \right\} = \sigma' \ell - \bar{E} + \epsilon' \ell f - \frac{e \frac{\partial \bar{E}}{\partial t}}{h}$$

Since the electromagnetic boundary-value problems presented by the model and the original are to be similar, we can determine how ϵ , μ , and σ must transform by requiring that the coefficients of

$$\frac{\partial \bar{H}}{\partial t}, \bar{E}, \text{ and } \frac{\partial \bar{E}}{\partial t}$$

be identical in both model and original.

Equating the coefficients in Equations (12b) to those in Equations (9), three obviously independent relations result

$$\begin{aligned} \mu &= \mu' \ell f - \frac{h}{e} \\ \sigma &= \sigma' \ell - \frac{e}{h} \\ \epsilon &= \epsilon' \ell f - \frac{h}{e} \end{aligned} \quad (13a)$$

For simplicity of notation, since ℓ , f , e , and h are ratios of model to original sizes, frequencies, \bar{E} and \bar{H} fields, respectively, we now redefine ϵ , μ , and σ to be ratios of model permittivity, permeability, and conductivity to those of the original.

Then, the above three equations take the simpler form

$$\begin{aligned}
 \frac{\mu f}{e} &= 1 \\
 \frac{\sigma l}{h} &= 1 \\
 \frac{\epsilon lf}{h} &= 1
 \end{aligned} \tag{13b}$$

and involve the seven variables

$$\epsilon, \mu, \sigma, l, f, \text{ and } \frac{e}{h}$$

Since the \bar{E} and \bar{H} field coefficients only appear as a ratio, we then define

$$\zeta = \frac{e}{h} \tag{14}$$

which is actually the ratio of model impedances to those in the original, and our three equations take the final form

$$\mu lf = \zeta \tag{15a}$$

$$\sigma l \zeta = 1 \tag{15b}$$

$$\epsilon lf \zeta = 1 \tag{15c}$$

in a total of six variables.

SOLUTIONS OF THE MODELING EQUATIONS

Complete solutions to the three nonlinear equations in six variables given in Equations (15) have not apparently been published. In practice, one seeks solutions for l , f , and ζ as functions of the parameters ϵ , μ , and σ available in actual materials used for models.

GENERAL SOLUTION

Eliminating ζ , the ratio of fields, from Equations (15) yields the three expressions

$$\mu\epsilon(\ell f)^2 = 1 \quad (16a)$$

$$\mu\sigma\ell^2 f = 1 \quad (16b)$$

$$\frac{\sigma}{\epsilon f} = 1 \quad (16c)$$

The first two are similar to Stratton's conditions for electrodynamic similitude [13], although arbitrary constants have been evaluated and no appeal is made to dimensionless measure numbers of the field variables.

The third equation is new, although it has often been stated that scaled model conductivity should be p times that in the original system [1, 4, 5, 8-11, 14-16, 18].

What has been untouched is other solutions of Equations (15) and the behavior of electromagnetic fields in physical scale models. Going back to Equations (15), and solving each of these expressions for ζ

$$\zeta = \mu\ell f \quad (17a)$$

$$\zeta = \frac{1}{\sigma\ell} \quad (17b)$$

$$\zeta = \frac{1}{\epsilon\ell f} \quad (17c)$$

However, the presence of all six variables in Equations (17) complicates interpretation.

On the other hand, if ℓ is eliminated from Equations (15), two new expressions result

$$\zeta = \sqrt{\frac{\mu}{\epsilon}} \quad (18a)$$

$$\zeta = \sqrt{\frac{\mu f}{\sigma}} \quad (18b)$$

A third is also produced which is actually the same as Equation (16c).

If f , last of the three variables, is eliminated from Equations (15), only one relation is produced, which is the same as Equation (18a).

This constitutes a complete set of solutions to the three nonlinear Equations (15), as can be seen by successively eliminating either ℓ , or f , or ζ from Equations (15) and finding all solutions for each of the remaining two variables as a function of the third and of the remaining three parameters ϵ , μ , and σ .

Equations (18) may have profound implications for physical scale models, because they provide a general solution relating ζ , the ratio of electric and magnetic fields as defined in Equation (14), to f and the three material parameters ϵ , μ , and σ . Equations (16), (17), and (18) will now be used to show how finite σ affects the surface currents and to discuss proper scaling of the electromagnetic fields and the scattering cross section, differences between geometric and complete scaling, and dependence of absorption and energy balance on f .

FINITE CONDUCTIVITY AND SURFACE CURRENTS

In practice, scale models are limited by values of ϵ , μ , and σ obtainable in model materials. For many measurements, ϵ' and μ' in the model will not differ appreciably from their values in the full-scale system. According to Equation (18a), the ratio of fields should also not differ appreciably in a completely scaled system.

However, if one uses Equation (14), definition of the impedance, in Equation (18b), one obtains

$$h = \frac{e}{\zeta} = e \sqrt{\frac{\sigma}{\mu f}} \quad (19)$$

which implies that, if σ (or, more properly, σ/μ) does not increase linearly with f , the ratio of \bar{H} fields shrinks with respect to the ratio of \bar{E} fields.

This is understandable because a σ not increasing fast enough for proper

scaling leads to diminished surface currents, which cause a decline in their associated \bar{H} fields.

The coupling between electromagnetic fields and surface currents is simple and direct.

For a perfect conductor, tangential \bar{E} at the surface is zero (otherwise, any surface current would be infinite), but tangential \bar{H} is finite, and the fields are damped waves that fall off infinitely rapidly with penetration into the metal, so \bar{H} and \bar{E} are both zero directly below the surface. Stokes's theorem implies a surface-current density, numerically equal to tangential \bar{H} , but at right angles to it, to account for the rapid decrease of tangential \bar{H} from its finite surface value to zero directly below the surface. This current can flow without a corresponding tangential \bar{E} because of the perfect conductivity.

Inside a good conductor, the transverse \bar{H} falls off rapidly as we penetrate the metal. This rapid change of \bar{H} with depth leads to a large $\bar{\nabla} \times \bar{H}$, and hence the Maxwell Equation (2a) implies a large current density \bar{J} , since conduction currents are much larger than displacement currents in a good conductor. Thus, there will be a large current flowing in a thin metal surface layer. By Ohm's law [Equation (7)], this surface current is parallel to \bar{E} and proportional to it, but the magnitude of \bar{E} is small for large values of σ . Since \bar{H} drops to zero well inside the conductor, Stokes's law implies the tangential component of \bar{H} just outside the metal surface equals the current flowing parallel to the surface, per unit length of surface.

In the limit of infinite conductivity, \bar{J} in the surface layer becomes infinite, but δ becomes zero in such a way that a finite current per unit length of surface results, which is numerically equal to the tangential component of \bar{H} at the surface. On the other hand, tangential \bar{E} goes to zero all through the surface layer, so tangential \bar{E} at the surface is also zero.

In fact, when both target and model conductivity are infinite, so both metal surfaces are perfect reflectors for waves at all frequencies, then σ becomes the ratio of two infinities, which is indeterminate. Therefore, one general scaling equation, Equation (15b), becomes trivially satisfied, and the other two, Equations (15a) and (15c), have the simple solutions given in Equations (16a), (17a), (17c), and (18a). Furthermore, since ℓ and f appear only in the product (ℓf) in the general modeling Equations (15a) and (15c), if one assumes geometric scaling

$$\ell f = 1 \quad (20)$$

then, according to Equation (18a), the usual f -independence assumed for ϵ and μ will imply electromagnetic fields whose ratio ζ doesn't depend on f .

In addition, with Equation (20) used to link ℓ and f in the general modeling Equations (15a) and (15c), all dependence on both these variables disappears from their solutions, so no f -dependence of material properties is required for proper scaling.

On the other hand, with both target and model σ taken to be finite, additional requirements imposed by the general scaling equation, Equation (15b), lead to a patent f -dependence of material properties being needed for proper scaling that complicates the new solutions given in Equations (16b), (16c), (17b), (18b), and (19). To better understand this required f -dependence of material properties, it is helpful to consider the differences between geometric and complete scaling.

DIFFERENCES BETWEEN GEOMETRIC AND COMPLETE SCALING

In our notation, the geometric scaling condition is expressed by Equation (20). Increased f is then associated with decreased size, so a scaled target has the same dimensions in scaled wavelengths as the actual target has in actual wavelengths.

For realistic materials with finite σ , models built according to the geometric

scaling condition of Equation (20) lead to further conditions on the material properties involved if complete scaling is to prevail. These conditions can be neatly obtained by using Equation (20) to link ϵ and f in the general modeling Equations (15). This process permits elimination of ℓ . Solutions for ζ may then be obtained as functions of f and of the parameters ϵ , μ , and σ available in actual model materials.

Explicitly, using Equation (20) to eliminate ℓ from Equations (15), the three independent basic modeling relations simplify to

$$\begin{aligned}\zeta &= \mu \\ \sigma\zeta &= f \\ \epsilon\zeta &= 1\end{aligned}\tag{21}$$

Eliminating ζ from Equations (21) yields the analogues of Equations (16)

$$\begin{aligned}\mu\epsilon &= 1 \\ \sigma\mu &= f \\ \frac{\sigma}{\epsilon f} &= 1\end{aligned}\tag{22}$$

These are the conditions Maxwell's equations place on the materials needed for accurate simulation of systems by models. We see that various combinations of σ with ϵ and μ should increase linearly with f , while ϵ and μ also satisfy the first of Equations (22).

In Equations (21), no ℓ or f , common to more than one equation, can be eliminated there. However, solving each of Equations (21) for ζ , the analogues of Equations (17) are

$$\begin{aligned}
 \zeta &= \frac{\mu}{\epsilon} \\
 \zeta &= \frac{f}{\sigma} \\
 \zeta &= \frac{1}{\epsilon}
 \end{aligned} \tag{23}$$

and multiplying pairs of these yields the analogues of Equations (18)

$$\begin{aligned}
 \zeta &= \sqrt{\frac{\mu}{\epsilon}} \\
 \zeta &= \sqrt{\frac{\mu f}{\sigma}} \\
 \zeta &= \sqrt{\frac{f}{\sigma \epsilon}}
 \end{aligned} \tag{24}$$

Equations (24) are very similar to Equations (18), and again imply that a σ not increasing fast enough for proper scaling leads to diminished surface currents and declining \bar{H} fields.

CONDITIONS FOR AN ABSOLUTE MODEL

Sinclair [5] also discussed modeling theory for electromagnetic systems. Since there are only four fundamental units (mass, length, time, and charge), four scale factors should suffice to describe any electromagnetic quantity. Thus, he introduced four factors to relate full-scale length, frequency (or time), \bar{E} , and \bar{H} , to model quantities, analogous to those in Equations (10) and (11).

He derived three equations similar to Equations (13a), intending to absolutely replicate a full-scale system, with both geometries and field strengths being modeled. He then calculated how 24 quantities [including Poynting vector and radar cross section (RCS)] transform as functions of the four scale factors, and claimed he could obtain quantitative data on all electromagnetic properties of a system,

including absolute power levels as well as configurations of lines of force.

However, Maxwell's equations fix only the ratio $\zeta = e/h$, and not e or h , separately. Thus, Sinclair simply noted that if a specific value is assigned to either e or h , his model is absolute and will yield quantitative results for all quantities. Otherwise, his model is a geometric one.

Many scale models are built to satisfy the geometric scaling condition of Equation (20), so one cannot then deduce power levels directly from model measurements. However, absolute values can be obtained by measuring relative power in the model system and calibrating this power by comparing signals returned from a model with those from a target of known RCS.

Unfortunately, Sinclair [5] provided no general solutions of the modeling equations, and did not consider effects of differences between geometric and complete scaling on electromagnetic fields, nor the influence of finite σ on surface currents. Also, little attention was paid to dependence on frequency.

ABSORPTION IN NONDISPERSIVE TARGETS

The scaling laws considered above imply replication of each field coefficient in the Maxwell Equations (9), considered separately, and consist of three general nonlinear modeling Equations (15) in the six ratios: ℓ , f , ζ , ϵ , μ , and σ . However, now going back to the original meaning of ϵ , μ , and σ (and f), while their static values are reasonably well known, absorption at higher frequencies occurs near eigenfrequencies of the molecular or electronic vibrations causing \bar{P} or \bar{M} polarization of materials.

At these frequencies, the linear constitutive Equations (6) and Ohm's law, Equation (7), are not valid. The values of these eigenfrequencies depend on the substance concerned, and vary widely, but become important whenever ϵ , μ , and σ exhibit the f -dependence known as dispersion. Moreover, since the presence of

dispersion in general signifies a dissipation of energy, nearness to these eigenfrequencies is also indicated whenever materials absorb. Thus, a dispersive medium is also an absorbing medium. In addition, the frequencies at which dispersion phenomena first appear may be entirely different for the electric and magnetic properties of a substance, as well as being dependent on direction in the lattice. In this report, while we continue to acknowledge anisotropy, we defer its proper treatment until a future time.

Since absorption at higher frequencies occurs near eigenfrequencies of the molecular or electronic vibrations causing \bar{P} or \bar{M} polarization of materials, one would expect this absorption to be associated with λ for the electromagnetic fields eventually becoming comparable with atomic dimensions, so the macroscopic formulation utilized above is invalid. On the contrary, there is an extensive frequency range in which absorption and dispersion phenomena are important but, fortunately, λ for electromagnetic fields is much larger than that of atomic or molecular dimensions, so a macroscopic formulation utilizing ϵ , μ , and σ is appropriate.

The quantum-mechanical band structure of solids shows that conductors have "free" electrons in partially filled bands, while insulators have bands filled to the full extent permitted by the Pauli principle. In conductors, these "free" electrons have their motion damped by collisions involving momentum transfers to the atoms making up the resistive medium, lattice imperfections, and impurities. This electron inertia usually is felt at a lower frequency than any resonant absorption frequency, and is then the first cause of dispersion. The Drude theory explains these dispersive effects of electron inertia by means of a complex ϵ [19, 24]. Hence, it is quite proper to consider nondispersive absorption up through microwave frequencies to the range where the effects of electron inertia begin to be felt.

ELECTRIC AND MAGNETIC SCATTERING

Since both the physical causes and mathematical formulation of electric and magnetic scattering are quite different, each type of scattering can be considered separately.

Electric Scattering

For nondispersive materials with real ϵ and σ , typical electric absorption would take place in a lossy dielectric, whose parameters satisfy the Maxwell curl equation

$$\nabla \times \bar{H} = \sigma \bar{E} + \epsilon \frac{\partial \bar{E}}{\partial t} \quad (9b)$$

The two terms on the right hand side of Equation (9b) represent conduction and convection currents, which depend on frequency. However, any variable field can be Fourier transformed into a series of single-frequency components, in which all quantities depend on time through the complex exponential factor $\exp(i\omega t)$. This form makes it possible to reduce operations of time differentiation to simple multiplication by $i\omega$, and also to more readily consider all parameters of equations as complex variables.

Assuming an $\exp(i\omega t)$ time dependence, monochromatic fields are singled out, and Equation (9b) becomes

$$\nabla \times \bar{H} = \sigma \bar{E} + i\epsilon\omega \bar{E} \quad (25a)$$

whereupon it can be seen that the conduction and convection currents are 90 degrees out of phase. The ω dependence apparent on the right hand side implies that the resistive conduction current dominates at lower ω , whereas the reactive convection current dominates at higher ω .

If σ is considered to be the seat of all electric losses, it is convenient to define a quantity n called the (electric) loss tangent

$$\eta = \frac{\sigma}{\omega\epsilon} = \frac{\text{conduction current density}}{\text{displacement current density}} \quad (26)$$

Since η is obviously a function of frequency, then the degree to which a material exhibits conductor or dielectric properties depends on frequency. More specifically,

$$\eta \left\{ \begin{array}{ll} \gg 1 & \text{conductor} \\ \ll 1 & \text{dielectric} \end{array} \right.$$

On the other hand, scaling of σ and ϵ according to Equations (13a), which insures proper replication of each coefficient of the Maxwell equations, leads to a loss tangent not changing with frequency, so the degree to which a properly scaled material exhibits the properties of a conductor or dielectric should not change with frequency.

Magnetic Scattering

Typical magnetic absorption occurs in magnetized ferrites, which can be very anisotropic (e.g., directional couplers) and whose parameters may show strong nonlinearity in their dependence on the magnitude of \bar{H} . However, the right-hand side of the other Maxwell curl equation

$$\bar{\nabla} \times \bar{E} = -\mu \frac{\partial \bar{H}}{\partial t} \quad (9a)$$

consists of only one term.

Assuming a time dependence of the form $\exp(iwt)$, monochromatic fields are again singled out, and Equation (9a) becomes

$$\bar{\nabla} \times \bar{E} = -i\mu\omega\bar{H} \quad (25b)$$

whereupon it can be seen that nondispersive materials with real μ have no room for magnetic absorption. However, magnetic absorption will occur in dispersive materials when μ acquires an imaginary part. The imaginary part of μ then plays a

role in Equation (25b) analogous to that of σ in Equation (25a), so it becomes possible to define a magnetic loss tangent that is the ratio of two current densities like those in Equation (26).

However, for nondispersive materials with real μ , there is no magnetic conduction current, as well as no free magnetic charge, and the magnetic loss tangent is zero at all frequencies.

Furthermore, scaling of μ according to Equations (13a) does not allow for magnetic absorption here at any frequency.

PLANE WAVES IN DISSIPATIVE MATERIALS

The electric and magnetic properties of materials both influence the reflection and absorption of electromagnetic waves by targets. We now consider how the reflection coefficient and radar cross section (RCS) change as frequency increases, and as incomplete scaling causes n to decrease through the value $n = 1$ [13, 19, 25].

Both \bar{E} and \bar{H} satisfy (damped) wave equations of the same form. Taking the curl of Equation (9a), substituting from Equation (9b) for $\bar{\nabla} \times \bar{H}$, and assuming no free charges on surfaces, yields

$$\nabla^2 \bar{E} - \sigma\mu \frac{\partial \bar{E}}{\partial t} - \epsilon\mu \frac{\partial^2 \bar{E}}{\partial t^2} = 0 \quad (27a)$$

An analogous procedure yields an identical equation for \bar{H} .

In a rectangular coordinate system, for incident uniform plane waves normal to a surface at $z = 0$, the solution of Equation (27a) takes the form

$$\bar{E} = \bar{E}_0 \exp(iwt - Yz) \quad (28)$$

where \bar{E}_0 is a constant amplitude vector in the direction of the wave's polarization, and Y is the complex propagation constant. Inserting Equation (28) into Equation (27a) yields

$$\begin{aligned} Y^2 &= i\omega\mu(\sigma + i\omega\epsilon) \\ &= -\omega^2\epsilon\mu(1 - in) = -k^2(1 - in) \end{aligned} \quad (29)$$

Thus, Y is actually a function of only two parameters: (a) k , the propagation constant of light when $\sigma = 0$

$$k = \frac{\omega\sqrt{\epsilon\mu}}{v} = \frac{2\pi}{\lambda} \quad (30)$$

where v is the velocity of light in a material medium ($v = 1/\sqrt{\epsilon\mu}$), and (b) the electric loss tangent n from Equation (26).

By taking the square root of Equation (29), Y itself can be written as a sum of the proper real (α) and imaginary (β) parts

$$Y = \alpha + i\beta \quad (31)$$

to make Equation (28) a solution of Equation (27a). The nonnegative character of ϵ , μ , and σ causes Y^2 to lie in the second quadrant of the complex plane, so its positive square root lies in the first quadrant, and thus α and β have the same sign. The other square root would be denoted by $-Y$.

Substituting expressions of the form of Equation (28) for \bar{E} and \bar{H} into Maxwell's equations, the plane wave considered is polarized, with \bar{E} and \bar{H} at right angles to each other and to the direction of propagation. The wave (or characteristic) impedance Z of a medium is defined as the ratio of the magnitude of \bar{E} to the magnitude of \bar{H} , where

$$\begin{aligned} Z^2 &= \frac{i\omega\mu}{\sigma + i\omega\epsilon} \\ &= \frac{\mu}{\epsilon} \frac{1}{(1 - in)} = (Z_0)^2 \frac{1}{(1 - in)} \end{aligned} \quad (32)$$

Thus, Z also turns out to be a function of two parameters: (a) Z_0 , the characteristic impedance of a medium when $\sigma = 0$

$$Z_0 = \sqrt{\frac{\mu}{\epsilon}} \quad (33)$$

which reduces to 376.6Ω for free space, and (b) the electric loss tangent η from Equation (26).

By taking the square root of Equation (32), Z itself can also be written as a sum of real (Z') and imaginary (Z'') parts

$$Z = Z' + iZ'' \quad (34)$$

where Z has the dimensions of a resistance. Since it, like γ , is complex in a conducting medium, there is in general a phase angle between the time dependence of \bar{E} and \bar{H} . The nonnegative character of ϵ , μ , and σ now causes Z^2 to lie in the first quadrant of the complex plane, so its positive square root lies in the first octant, and thus Z' and Z'' have the same sign.

The properties of the medium may be neatly expressed in terms of γ and Z , allowing the two Fourier-transformed Maxwell curl Equations (25a) and (25b) to be written

$$\bar{\nabla} \times (Z\bar{H}) = -\gamma\bar{E} \quad (35a)$$

$$\bar{\nabla} \times \bar{E} = -\gamma(Z\bar{H}) \quad (35b)$$

From them, as with Equation (27a), we may derive the wave equations

$$\nabla^2\bar{E} - \gamma^2\bar{E} = 0 \quad (27b)$$

$$\nabla^2\bar{H} - \gamma^2\bar{H} = 0 \quad (27c)$$

satisfied by all components of \bar{E} and \bar{H} .

All solutions of Equations (27b), (27c), and (35) are thus functions of only γ and Z , and therefore of the three parameters: k , Z_0 , and η , as given by Equations (30), (33), and (26), respectively. It is often convenient to use the Maxwell equations and the wave equations in these forms.

SCALING OF THE SCATTERING CROSS SECTION

Since all solutions of the Fourier-transformed wave and Maxwell equations for

\bar{E} and \bar{H} , Equations (27b), (27c), and (35), are functions only of Y and Z , and therefore of the three parameters k , Z_0 , and n , investigating the scaling of any quantity derived from the \bar{E} and \bar{H} fields reduces to investigating the scaling of these three quantities, given by Equations (30), (33), and (26), respectively.

For nondispersive materials, neither ϵ' nor μ' will differ from their values in the full-scale system. As we have seen from Equations (18) and (24), the ratio of fields should also not differ in a completely scaled system. Thus, Z_0 should not change with frequency.

Equations (22) are the conditions Maxwell's equations place on the materials needed for accurate simulation of systems by models. If neither ϵ' nor μ' differ from their values in the full-scale system, the first of Equations (22) is automatically satisfied, and the second and third of Equations (22) both imply that σ should increase linearly with f . Therefore, neither n nor Z should change with frequency in a completely scaled system.

Thus, under complete scaling, neither Z , Z_0 , nor n will change with frequency, while Y and k both can easily be seen from Equations (29) and (30) to increase linearly with f .

On the other hand, for the special case of a uniform plane wave normally incident from free space (medium 1) upon the plane surface of a dissipative block (medium 2), such generality is not necessary.

In medium 1, \bar{E} consists of incident and reflected waves, and one defines a reflection coefficient R , measuring the amplitude ratio of reflected to incident \bar{E} . In medium 2, there is also a transmitted wave, so one can define a transmission coefficient T , analogous to R . Both Stratton [13] and Adler et al. [25] calculated R and T for scattering from dissipative surfaces and found that both these coefficients depend only on the Z 's and not on the Y 's.

Thus, under complete scaling, since both R and T depend on the Z 's and not on

the Υ 's, although the scaled RCS of a target will decrease as the square of increasing frequency (like a physical area), its properly scaled reflection coefficient should not change.

On the other hand, under incomplete scaling, with the scatterer's μ , ϵ , and σ not regarded as functions of frequency, and with medium 1 being free space with loss tangent zero, the only remaining f-dependence resides in n for medium 2, which is also a function of the values of σ and ϵ there.

ENERGY BALANCE AND DEPENDENCE ON FREQUENCY

It is physically impossible to satisfy scaling conditions on σ when good conductors like copper or aluminum are used in the original system and the frequency change is appreciable because, for copper and aluminum, σ is so near the theoretical maximum that it cannot be increased in accordance with Equations (16c) and (18b). However, water, resistive conductors, and lossy dielectrics have conductivities far enough from the theoretical maximum that their σ can be increased in accordance with Equations (16c) and (18b) for appropriate changes in f . Experience with more severe requirements in obtaining materials with necessary σ is found in geophysical applications, where p in Equation (10b) must be of order 200 to 1000 for modeling mineral prospecting problems and perhaps as large as 100,000 to 1,000,000 to study effects of large-scale structures on geomagnetic variations [8].

On the other hand, little concern has been shown about scaling σ in radar applications [1], if the model is a metal of high σ , since it is felt that high σ models have only a small surface component of \bar{E} , and differences between the surface current distribution on a poor conductor and that on a perfectly conducting target have been believed to be unimportant.

However, a simple argument based on Equation (19) leads to quite different

predictions. For a plane wave incident on a physical scale model, electric and magnetic energy densities are equal to each other outside the conductor, and the radar cross section (RCS) comes equally from both electric and magnetic scattering. Therefore, if the ratio of scattered \bar{H} fields shrinks with respect to the ratio of \bar{E} fields in accordance with Equation (19), then measured values of the RCS of scaled targets should approach one-half the value predicted for an ideal model.

Actually, magnetic losses are twice as important as the above argument would indicate. Inside the conductor, the time average of the electrical energy density is $\epsilon\bar{E}^2/2$, while that associated with the \bar{H} fields is $\sigma\bar{E}^2/2\omega$, so their ratio is $\epsilon\omega/\sigma$, which is assumed small in agreement with Equation (26). Therefore, the energy density in a conductor is predominantly magnetic, so good conductors are essentially not penetrated by \bar{E} fields satisfying the condition that $\epsilon\omega \ll \sigma$. Thus, instead of measured values of the RCS of incompletely scaled targets approaching one-half the value predicted for an ideal model, the diminished surface currents and declining \bar{H} fields associated with a σ not increasing fast enough with frequency for proper scaling lead to a ratio of measured values of the RCS to that predicted for an ideal model which will eventually vanish [26].

These general concepts remain valid in variable electromagnetic fields, even if dispersion is present [27]. Because of the continuity of the tangential components of \bar{E} and \bar{H} , the normal component of \bar{S} in Equation (8b) is continuous at the boundary of a body, and the interpretation of \bar{S} as an energy flux density carries over from a vacuum, across surfaces, into more complicated bodies. However, in the presence of dispersion, the interpretation of energy density is more complicated, because the presence of dispersion generally signifies dissipation of energy, since a dispersive medium is also an absorbing one.

SUMMARY AND CONCLUSIONS

Since, all scattering characteristics, including interference and diffraction, polarization, and creeping and traveling (surface) wave phenomena, should be correctly represented by rigorous scale modeling, the distribution of radiation scattered from a full-size target is expected to be predictable from measurements on a faithful scale model.

Therefore, a complete and rigorous treatment of the predictions of electrodynamic similitude relating scattering from scaled and full-size targets was developed, starting with the usual assumption that ϵ , μ , and σ do not change with f . Three general nonlinear modeling equations in six variables were derived, and a complete set of solutions was presented. Scaling laws for such models explicitly involve ϵ , μ , and σ . However, practical difficulties with scaling properties of realistic materials now exist which, for most scattering measurements, have discouraged all but simple geometric scaling.

Particular emphasis was given to the effects of differences between geometric and complete scaling on the electromagnetic fields and on the radar cross section (RCS), and the effects of approximations to complete scaling were evaluated. Conditions were obtained on properties of materials required for models made from these materials to accurately simulate systems. Absorption and energy balance were also treated, and the influence of finite σ on surface currents was shown.

Scaling laws are the result of exact conditions on each coefficient of Maxwell's equations. Since the claim that scaled-down models may be used to represent real targets is based on linearity of Maxwell's equations, we also examined the physics involved in nonlocality and nonlinearity, its relation to the Maxwell equations in macroscopic media, and its impact on physical scale modeling. Nonlocality in space may often be neglected in conductors up through optical frequencies, as long as the mean free path for conduction electrons is small, and

the radar wavelength is large, compared to the skin depth. When these conditions are satisfied, ϵ , μ , and σ become functions only of f in dispersive targets.

The behavior of electromagnetic fields was also examined as a function of f . If σ were infinite, as is usually assumed, satisfying general scaling requirements would be elementary, because all solutions to the general modeling equations are then trivially satisfied, except those leading to geometric scaling.

Unfortunately, it is physically impossible to satisfy scaling conditions exactly when realistic materials are used and the change in f is appreciable, because this would require that upper bounds on physical σ be exceeded at higher f , and definite limitations also exist on physical ϵ and μ .

This paper showed that incomplete scaling of apparently nonabsorptive targets may have profound implications for model measurements. Both electric and magnetic scattering were considered. All the energy density in the reflected wave may be lost at higher f , and the ratio of the measured RCS of geometrically scaled targets to that predicted for a completely scaled model will eventually approach zero.

RECOMMENDATIONS

Even though we have concentrated on scattering of radar waves from targets, very few conclusions actually depending on properties of waves have been used, beyond Equation (20). To assess effects of compromises with complete scaling, a more realistic calculation of the precise interaction of electromagnetic waves with physical models is needed.

First, the scattering amplitude should be calculated for electromagnetic waves impinging on nondispersive materials in the proper frequency domain with a more careful description of fields and currents. Such a description is quite applicable up through microwave frequencies to the range where the effects of electron inertia begin to be felt. Both reflection and absorption coefficients should be

calculated, as well as phase angles. Ratios of the measured radar cross section (RCS) values of scaled targets to those predicted for an ideal nondispersive model should also be calculated.

These calculations should be extended to dispersive materials up through higher microwave frequencies into the range where the effects of electron inertia can be felt. In general, as f increases up through the modeling range, and becomes comparable with frequencies corresponding to electron-lattice interactions and to electron motion within atoms and molecules of the material media (optical frequencies), absorption takes place, which leads to μ , ϵ , and σ becoming complex functions of f with real and imaginary (reflective and absorptive) parts.

The gradual onset of absorption in good conductors as f increases through the modeling range permits a simple description in terms of electron inertia. In conductors, electron inertia is usually felt at a lower f than other forms of absorption, and is also the first cause of dispersion. The Drude theory describes these dispersive effects of electron inertia well with a complex ϵ , and can be applied to metals as σ decreases with increasing f through the modeling range from the X-band used on full-scale ships to the shortest λ considered for physical scale models. Ratios of the measured RCS values of scaled targets to those predicted for such a dispersive model should also be calculated and compared with those obtained for the nondispersive case.

ACKNOWLEDGMENTS

The author is thankful to Drs. R.C. Allen and A. Powell and to R.H. Burns, J.R. Crisci, M. Greenberg, G.M. Remmers, and G.C. Switzer for encouragement and support during this project. Dr. R.C. Allen particularly emphasized examining the surface currents. The author is also grateful to Drs. S.H. Brown, P.O. Cervenka, and B.R. Hood and to R.H. Burns, D.L. Etherton, and O.M. Pearcy for many helpful discussions.

REFERENCES

1. Corriher, H.A., "RCS Measurements on Scale Models," In: Techniques of Radar Reflectivity Measurement, Nicholas C. Currie, Ed., Artech House, Dedham, MA (1984), Ch. 10, pp. 329-374
2. Abraham, M., "Ein Satz über Modelle von Antennen," Mittlg. der Phys. Ges. Zurich, Vol. 19, pp. 17-20 (1919), as given in Reference 6.
3. Raymond, R.C., "Scattering of 10 cm Radiation by a Model Airplane," Massachusetts Institute of Technology Radiation Laboratory Report RL-156, ATI 45 262 (21 May 1942), as given in Reference 1.
4. Sinclair, G., E.C. Jordan, and E.W. Vaughan, "Measurement of Aircraft-Antenna Patterns Using Models," Proc. Inst. Radio Eng., Vol. 35, pp. 1451-1462 (1947).
5. Sinclair, G., "Theory of Models of Electromagnetic Systems," Proc. Inst. Radio Eng., Vol. 36, pp. 1364-1370 (1948).
6. Blacksmith, P., Jr., R.E. Hiatt, and R.B. Mack, "Introduction to Radar Cross-Section Measurements," Proc. Inst. Electrical Electronics Eng., Vol. 53, pp. 901-920 (1965).
7. Bahret, W.F., and C.J. Sletten, "A Look into the Future of Radar Scattering Research and Development," Proc. Inst. Electrical Electronics Eng., Vol. 53, pp. 786-795 (1965).
8. Frischknecht, Frank C., "Electromagnetic Scale Modelling," In: Electromagnetic Probing in Geophysics, James R. Wait, Ed., The Golem Press, Boulder (1971), Ch. 8, pp. 265-320.
9. Cram, L.A., and S.C. Woolcock, "Development of Model Radar Systems between 30 and 900 GHz," The Radio and Electronic Engineer, Vol. 49, pp. 381-388 (1979).
10. Waldman, J., H.R. Fetterman, W.D. Goodhue, T.G. Bryant, and D.H. Temme,

"Submillimeter Modeling of Millimeter Radar Systems," Proc. Soc. Photo-Optical Instrumentation Eng., Vol. 259, pp. 152-157, Millimeter Optics Conf. in Huntsville, AL (1980).

11. Bachman, C.G., Radar Targets, D.C. Heath and Company, Lexington, MA (1982), Ch. 4, pp. 151-158.

12. Rohan, P., Surveillance Radar Performance Prediction, Peter Peregrinus Ltd., London (1983), Ch. 7, pp. 176-182.

13. Stratton, J.A., Electromagnetic Theory, McGraw-Hill BookCompany, New York (1941).

14. Brown, G.H., and Ronald King, "High-Frequency Models in Antenna Investigations," Proc. Inst. Radio Eng., Vol. 22, pp. 457-480 (1934).

15. King, R.W.P., Fundamental Electromagnetic Theory, Dover Publications, New York (1963), Ch. IV, pp. 316-320, [originally published as Electromagnetic Engineering, McGraw-Hill Book Company, New York (1945)].

16. Mentzer, J.R., Scattering and Diffraction of Radio Waves, Pergamon Press, New York (1955), Ch. 5, pp. 121-129.

17. Brown, D.H., R.J. Newman, A.L. Maffett, and J.W. Crispin,Jr., "Modeling Techniques," In: Methods of Radar Cross-Section Analysis, J.W. Crispin, Jr. and K.M. Siegel, Eds., Academic Press, New York (1968), Ch. 12, pp. 377-379.

18. Krichbaum, C.K., "Electromagnetic Models," In: Radar Cross Section Handbook, G.T. Ruck, D.E. Barrick, W.D. Stuart, and C.K. Krichbaum, Eds., Plenum Press, New York (1970), Ch. 11, pp. 900-934.

19. Jackson, J.D., Classical Electrodynamics, Second Edition, John Wiley & Sons, New York (1975).

20. Stern, F., "Elementary Theory of the Optical Properties of Solids," In: Solid State Physics, Vol. 15, F. Seitz and D. Turnbull, Eds., Academic Press, New

York (1963), Ch. 4, pp. 299-408.

21. Pippard, A.B., The Dynamics of Conduction Electrons,

Gordon and Breach, New York (1965).

22. Panofsky, W.K.H., and M. Phillips, Classical Electricity and Magnetism, Second Edition, Addison-Wesley Publishing Company, Reading, Massachusetts (1962).

23. Baldwin, G.C., Introduction to Nonlinear Optics, Plenum Press, New York (1969).

24. Schumacher, C.R., "The Interaction of Electromagnetic Energy with Physical Scale Models, Part II: Dispersive Targets with Electron Inertia Treated by the Drude Theory," DTNSRDC report (in preparation).

25. Adler, R.B., L.J. Chu, and R.M. Fano, Electromagnetic Energy Transmission and Radiation, John Wiley & Sons, New York (1960), Ch. 8, pp. 402-492.

26. Schumacher, C.R., "The Interaction of Electromagnetic Energy with Physical Scale Models, Part I: Nondispersive Targets," DTNSRDC report (in preparation).

27. Schumacher, C.R., "Electrodynamic Similitude and Physical Scale Modeling, Part II: Dispersive Targets," DTNSRDC report (in preparation).

INITIAL DISTRIBUTION

Copies	Copies
1 DARPA	NAVSEA (Cont)
2 CNO	1 PMS 300
1 Code 351 (CAPT R. Allen)	1 PMS 399
1 Code 376 (CAPT R. Barr)	1 PMS 400
5 OCNR	1 NAVAIR (C. Thomas)
1 Code 111 (T.G. Berlincourt)	1 NWC (J.M. Bennett, Code 38103)
1 Code 1112 (B.R. Junker)	2 COMSPAWARSCOM
1 Code 1112 (M.F. Shlesinger)	1 (S. Edwards)
1 Code 1114 (K.L. Davis)	1 (L.I. Moskowitz)
3 ONT	2 NOSC
1 (J. Kelley)	1 Code 161 (D. Washburn)
1 Code 075 (CAPT W.C. Miller)	1 Code 161 (M. Prickett)
1 Code 075 (CDR P. Pierpont)	3 NSWC
10 NRL	1 L.L. Hill (D)
1 Code 2600 (TID)	1 E.J. Shuler (DG20)
1 Code 4700 (S. Ossakow)	1 S.E. McGonegal (H24)
1 Code 5310 (G.V. Trunk)	1 NADC (K. Foulke)
1 Code 5314 (H. Toothman)	1 NAVPGSCOL (L. Wilson)
1 Code 5360 (D. Kerr)	12 DTIC
1 Code 5370 (T.L. Cheston)	1 Professor Kenneth K. Mei
1 Code 5700 (J. Montgomery)	Electrical Engineering Dept
1 Code 5750 (G. Friedman)	University of California
1 Code 5753 (D.W. Forester)	Berkeley, CA 94720
	1 Professor Henry D.I. Abarbanel
22 NAVSEA	Scripps Institute of Oceanography
1 SEA 05 RADM M.V. Ricketts)	University of California, A-013
1 SEA 05R (J.E. Gagorick)	La Jolla, CA 92093
1 SEA 05R (C.A. Zanis)	1 Professor Edmund K. Miller
2 SEA 05R22 (A. Johnson)	Lawrence Livermore National Lab/
1 SEA 05R25 (H. Vanderveldt)	University of California, Box 5504
1 SEA 50 (CAPT B. Tibbetts)	Livermore, CA 94550
1 SEA 5031 (W.D. Bauman)	1 Professor Jeremy A. Landt
1 SEA 55 (CAPT R. Nutting)	Los Alamos Scientific Lab/
1 SEA 55X1 (J. Schell)	University of California,
2 SEA 55X12 (T. Ulinski)	Trinity Dr, Box 1663
1 SEA 55X12 (J. Traylor)	Los Alamos, NM 87544
1 SEA 56D5 (CDR E. Runnerstrom)	
1 SEA 61R4 (H.J. Demattia)	
1 SEA 61XB (CAPT S. Pryzby)	
1 SEA 61X2 (N. Yannarell)	
1 SEA 62AT (R.J. Hill)	
1 SEA 91	

Copies	Copies
1 Professor Herbert M. Uberall Physics Department Catholic University of America Washington, DC 20064	1 Professor Thomas B.A. Senior Electrical Engineering Dept University of Michigan Ann Arbor, MI 48109
4 Modeling & Analysis Division Engineering Experiment Station Georgia Institute of Technology Atlanta, GA 30332 1 Michael T. Tuley 1 Margaret M. Horst 1 John W. Peifer 1 R. Bruce Rakes	1 Professor Walter D. Burnside Electro Science Laboratory Ohio State University Columbus, OH 43212
1 Professor Donald R. Wilton Electrical Engineering Dept University of Houston Houston, Texas 77004	1 Professor Ercument Arvas Electrical Engineering Dept Rochester Institute of Technology Rochester, NY 14623
1 Professor P.L.E. Uslenghi Electrical Engineering Dept University of Illinois Chicago, IL 60680	1 Professor Kenneth J. Harker STAR Lab/Durand 207 Stanford University Stanford, CA 94305
1 Professor Raj Mittra Electrical Engineering Dept University of Illinois Urbana, IL 61801	1 Professor Roger F. Harrington Electrical Engineering Dept Syracuse University Syracuse, NY 13210
1 Professor Brian R. Judd, Chairman Dept of Physics Johns Hopkins University Baltimore, MD 21218	1 Professor Philip L. Marston Dept of Physics Washington State University Pullman, WA 99164
1 Professor Jerry Waldman Electrical Engineering Dept University of Lowell Lowell, MA 01854	
1 Professor Chuan Sheng Liu, Chairman Dept of Physics & Astronomy University of Maryland College Park, MD 20742	
1 Professor Robert E. McIntosh Dept of Physics & Applied Physics University of Massachusetts Amherst, MA 01002	

CENTER DISTRIBUTION

Copies	Code	Name
1	00	CAPT G.R. Garritson
1	01	R. Metrey
1	012.2	B. Nakonechny
1	012.3	D. Moran
1	012.4	R.L. Schaeffer
1	04	CAPT C.N. Calvano
1	12	W.C. Dietz
1	1202	G.M. Remmers
1	1202	P.J. Granum
1	1222	G.W. Peters
1	1231	M.A. Sekellick
1	1561	J.F. Dalzell
1	1730.4	M.O. Critchfield
1	184	J.W. Schot
1	1902	G. Maidanik
1	27	R.C. Allen
1	2702	W.J. Levedahl
1	2712	S.H. Brown, Jr.
1	2740.1	J.W. Dickey
1	2751	B.R. Hood
1	28	G.A. Wacker
1	2801	J.R. Crisci
1	283	H.H. Singerman
1	2833	M. Greenberg
1	29	G.G. Switzer
1	2901	R.G. Stilwell
1	2909	F. Gilchrist
1	293	R.H. Burns
1	293	O.M. Pearcy
1	293	D.L. Etherton
10	293	C.R. Schumacher
1	296	P.O. Cervenka
1	5211	M. Knox
10	5211.1	Repts Distribution
1	522.1	TIC (Carderock)
1	522.2	TIC (Annapolis)
2	5231	Office Services

DTNSRDC ISSUES THREE TYPES OF REPORTS

- 1. DTNSRDC REPORTS**, A FORMAL SERIES, CONTAIN INFORMATION OF PERMANENT TECHNICAL VALUE. THEY CARRY A CONSECUTIVE NUMERICAL IDENTIFICATION REGARDLESS OF THEIR CLASSIFICATION OR THE ORIGINATING DEPARTMENT
- 2. DEPARTMENTAL REPORTS**, A SEMIFORMAL SERIES, CONTAIN INFORMATION OF A PRELIMINARY, TEMPORARY, OR PROPRIETARY NATURE OR OF LIMITED INTEREST OR SIGNIFICANCE. THEY CARRY A DEPARTMENTAL ALPHANUMERICAL IDENTIFICATION.
- 3. TECHNICAL MEMORANDA**, AN INFORMAL SERIES, CONTAIN TECHNICAL DOCUMENTATION OF LIMITED USE AND INTEREST. THEY ARE PRIMARILY WORKING PAPERS INTENDED FOR INTERNAL USE. THEY CARRY AN IDENTIFYING NUMBER WHICH INDICATES THEIR TYPE AND THE NUMERICAL CODE OF THE ORIGINATING DEPARTMENT. ANY DISTRIBUTION OUTSIDE DTNSRDC MUST BE APPROVED BY THE HEAD OF THE ORIGINATING DEPARTMENT ON A CASE BY CASE BASIS.

END

DTIC

6 - 86